


Article

Gumbel (EVI)-Based Minimum Cross-Entropy Thresholding for the Segmentation of Images with Skewed Histograms

Walaa Ali H. Jumiawi *  and Ali El-Zaart

Department of Mathematics and Computer Science, Faculty of Science, Beirut Arab University,
Beirut 11072809, Lebanon; elzaart@bau.edu.lb

* Correspondence: walaali@hotmail.com

Abstract: In this study, we delve into the realm of image segmentation, a field characterized by a multitude of approaches; one frequently used technique is thresholding-based image segmentation. This process divides intensity levels into different regions based on a specified threshold value. Minimum Cross-Entropy Thresholding (MCET) stands out as an independent objective function that can be applied with any distribution and is regarded as a mean-based thresholding method. In certain cases, images exhibit diverse structures that result in different histogram distributions. Some images possess symmetric histograms, while others feature asymmetric ones. Traditional mean-based thresholding methods are well-suited for symmetric image histograms, relying on Gaussian distribution definitions for mean estimations. However, in situations involving asymmetric distributions, such as left and right-skewed histograms, a different approach is required. In this paper, we propose the utilization of a Maximum Likelihood Estimation (MLE) of Gumbel's distribution or Extreme Value Type I (EVI) distribution for the objective function of an MCET. Our goal is to introduce a dedicated image-thresholding model designed to enhance the accuracy and efficiency of image-segmentation tasks. This model determines optimal thresholds for image segmentation, facilitating precise data analysis for specific image types and yielding improved segmentation results by considering the impact of mean values on thresholding objective functions. We compare our proposed model with original methods and related studies in the literature. Our model demonstrates better performance in terms of segmentation accuracy, as assessed through both unsupervised and supervised evaluations for image segmentation.

Keywords: images segmentation; minimum cross-entropy; Gumbel distribution; improving segmentation methods; skewed histogram; extreme value distribution (EVI)



Citation: Jumiawi, W.A.H.; El-Zaart, A. Gumbel (EVI)-Based Minimum Cross-Entropy Thresholding for the Segmentation of Images with Skewed Histograms. *Appl. Syst. Innov.* **2023**, *6*, 87. <https://doi.org/10.3390/asi6050087>

Academic Editors: Teen-Hang Meen and Friedhelm Schwenker

Received: 11 August 2023

Revised: 18 September 2023

Accepted: 25 September 2023

Published: 29 September 2023



Copyright: © 2023 by the authors. Licensee MDPI, Basel, Switzerland. This article is an open access article distributed under the terms and conditions of the Creative Commons Attribution (CC BY) license (<https://creativecommons.org/licenses/by/4.0/>).

1. Introduction

Image-processing approaches have evolved to perform image segmentation using pixel thresholding, region-based techniques, and boundary thresholding [1]. Thresholding-based image segmentation is a process that tends to separate intensity levels into two regions in a given image. Some thresholding methods, e.g., the Otsu method and Minimum Cross-Entropy Thresholding, are considered mean-based techniques [2–4], and the original versions of these methods rely on the definition of Gaussian distribution for the mean estimation for their objective functions; this approach deals with images as they have symmetric intensity levels.

In general, images can have various forms of intensity distribution depending on their original structure. In remote-sensing applications, optical imagery of water bodies has been used on regional and global scales for water mapping [5]. Such optical images, including the water body's surface, can have right-skewed histogram distributions, and these images typically include rivers and lakes with variations in intensity that are shaped by seasonal conditions [6]. On the other hand, left-skewed distributions appear in some images' histograms, e.g., in special cases in medical images such as those of dermoscopic

skin lesions and other types of images. For instance, in some medical images, the skewness of a histogram can be influenced by factors such as the image acquisition parameters. When Magnetic Resonance Imaging (MRI) a brain, the segmentation task is affected if the intensity dissimilarity between adjacent glioma regions is small; this challenge was solved using U-Net to propose attention layers for small-intensity dissimilarities [7]. Moreover, Computed Tomography (CT) scan images can indeed vary depending on multiple factors, including the stage and type of infection, while the proportion of infected pixels in CT images is small [8]. Images of these kinds often present similar segmentation challenges, particularly when employing mean-based thresholding techniques while adhering to the Gaussian definition for a mean estimation [9]. The performance of mean-based thresholding methods in achieving superior segmentation results can be influenced by the choice of the probability distribution. For instance, the Gaussian distribution tends to perform optimally when dealing with symmetric intensity levels, whereas the utilization of the log-normal distribution can lead to improved mean estimations in cases involving right-skewed intensity levels, ultimately enhancing the effectiveness of mean-based objective functions [10]. However, Gumbel maximum and log-normal distributions do not necessarily have the same mean value, even for a right-skewed histogram. The mean value of a probability distribution is a measure of its central tendency and it can vary depending on the specific parameters of each distribution. The novelty of using the Gumbel distribution and Maximum Likelihood Estimation (MLE) lies in their ability to address these limitations effectively. Mitigating these limitations refines the thresholding function, improving the precision of image segmentation and target object detection, particularly in medical imaging and remote sensing.

The Gumbel distribution is commonly used for model estimation, and relies on mode and scale parameters. It encompasses two cases: the minimum (left-skewed), which is based on the smallest extreme value, and the maximum (right-skewed), which is based on the largest extreme value [11,12]. This paper introduces the use of a maximum likelihood estimation for Gumbel's distribution (both maximum and minimum) to estimate the mean in mean-based thresholding functions for skewed-histogram image segmentation. The contributions of this paper are as follows:

- The introduction of the utilization of the maximum likelihood estimation of the Gumbel distribution in thresholding methods.
- The proposal of an improved entropy-based thresholding model for the precise segmentation of images with skewed histograms and the validation of the results through unsupervised and supervised evaluations.
- The provision of an extended approach for mean estimations for both right- and left-skewed histograms.

The paper is organized as follows: Section 2 presents related works, along with an introduction to the Gumbel distribution. Section 3 explains the methodology, Section 4 discusses the performance evaluation, and Section 5 presents the discussion and results. Finally, Section 6 concludes the paper and outlines future work.

2. Related Work

Thresholding-based image segmentation methods have been frequently discussed in the literature. However, identifying the optimal threshold for precise segmentation continues to pose a significant challenge [13]. The simplest scenario for thresholding occurs when the input image $I(x, y)$ exhibits two distinct regions—the object and background—which are separated by a prominent valley in the corresponding image histogram. This scenario is known as a bimodal and symmetrical histogram in which the optimal threshold is positioned between these two regions, resulting in the creation of a segmented image $g(x, y)$ [14].

2.1. Minimum Cross-Entropy Thresholding (MCET)

MCET, introduced by Li et al. [3], is an entropy-based method for thresholding-based image segmentation. It features an independent objective function capable of employing any distribution for mean estimation. This flexibility arises from the original formulation of cross-entropy functions which was initially proposed by Kullback [15]. The optimization process hinges on the mean values within each region of the given image. Numerous entropy-based thresholding models have emerged to address data separation challenges [16–18]. The application of cross-entropy approaches has paved the way for advancements in image segmentation within the literature. MCET, for instance, was devised to separate agricultural data using previously estimated satellite imagery information [19]. Kapur’s entropy-based thresholding method found an application in water body segmentation [20]. To mitigate computational costs, a Particle Swarm Optimization (PSO)-based multilevel thresholding algorithm was proposed as an enhancement for MCET [21]. Additionally, the minimum cross-entropy method introduced improvements by utilizing the Gamma distribution to determine optimal thresholds [22]. Furthermore, the method was extended to multi-level threshold selection through an enhanced human mental search algorithm [23]. Concerning mean estimation for objective functions, mean-based thresholding methods, including MCET, have been enhanced through the integration of homogeneous and heterogeneous mean filter approaches [9,24]. MCET has been further developed by incorporating hybrid distributions in a parallel algorithm for image segmentation, including the utilization of Gaussian and Gamma distributions for skin lesion segmentation [25].

In this paper, we introduce the utilization of a Maximum Likelihood Estimation of the Gumbel distribution for mean-based thresholding methods, specifically for mean estimations within objective functions.

2.2. The Gumbel Distribution

The extreme value distribution Type I (EVI), or Gumbel’s distribution, was introduced by Gumbel [11]. It is used in hydrology for predicting extreme flood frequencies and rainfall rates. It also has a significant role in econometrics in modeling extreme changes in stock prices and interest rates [26,27]. The probability density function (PDF) of the Gumbel distribution has two cases: the maximum (skewed to the right distribution) or the minimum (skewed to the left distribution), as shown in (1) and (2), respectively.

$$f(x, \alpha, \beta) = \frac{1}{\beta} e^{-\frac{(x-\alpha)}{\beta}} e^{-e^{-\frac{(x-\alpha)}{\beta}}} \tag{1}$$

$$f(x, \alpha, \beta) = \frac{1}{\beta} e^{\frac{(x-\alpha)}{\beta}} e^{-e^{\frac{(x-\alpha)}{\beta}}} \tag{2}$$

Here, α and β represent the mode and scale parameters, respectively. The situation in which α equals 0 and β equals 1 is referred to as the standard Gumbel distribution. The probability density function (PDF) of the Gumbel distribution, in both its minimum and maximum forms, is graphically depicted in Figure 1. Various parameter selections have been made to generate these plots, illustrating the skewness of the Gumbel probability density function for both minimum and maximum scenarios.

2.3. Maximum Likelihood Estimation (MLE)

The MLE is known as asymptotical and impartial for Gumbel distribution. Nonetheless, it is not always optimal in small samples [11]. The MLE technique is to identify the most likely values of the mode and the scale parameter (α and β) for a given sample by maximizing the likelihood function.

$$L(\alpha, \beta) = \prod_{i=1}^n f(x, \alpha, \beta) \tag{3}$$

$\beta > 0, -\infty < x \text{ and } \alpha < \infty$

where L is the log-likelihood. Taking the first derivatives of (1) or (2), as shown in (4), yields

$$\frac{\partial \text{Log}(L(\alpha, \beta))}{\partial(\alpha, \beta)} = 0 \tag{4}$$

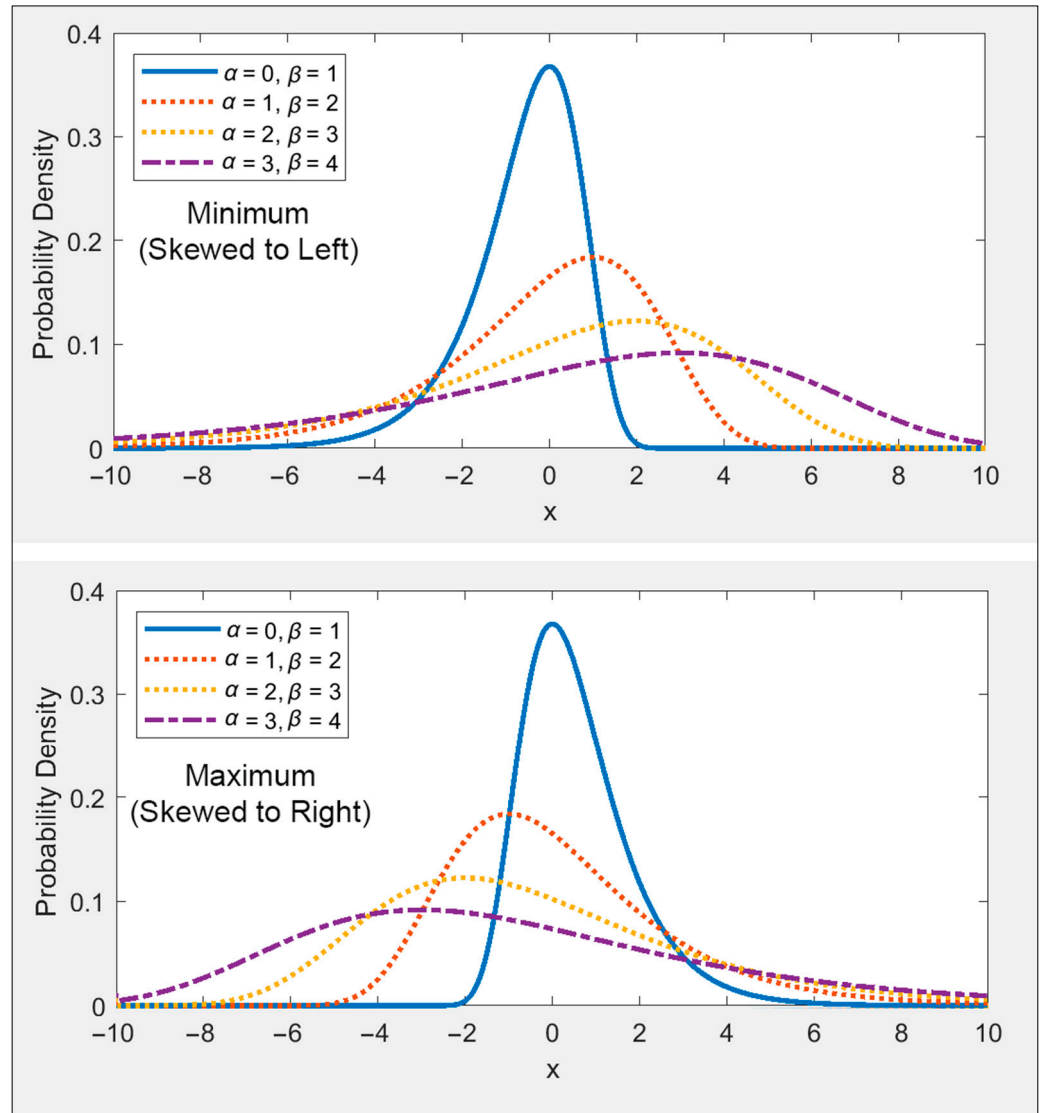


Figure 1. Samples of Gumbel probability density function for minimum and the maximum cases.

With regard to the parameters of any PDF, the output are two equations for α and β . The maximum likelihood estimators for the Gumbel distribution are given in [28,29]. The MLE of the minimum case is shown in (5) and (6). For the maximum case, values of x_i become negative.

$$\hat{\beta} = -\bar{x} + \frac{\sum_{i=1}^n x_i e^{\frac{x_i}{\hat{\beta}}}}{\sum_{i=1}^n e^{\frac{x_i}{\hat{\beta}}}} \tag{5}$$

$$\hat{\alpha} = -\hat{\beta} \text{Log} \left[\frac{1}{n} \sum_{i=1}^n e^{\frac{x_i}{\hat{\beta}}} \right] \tag{6}$$

where n and \bar{x} are the length and the mean of the given samples, respectively.

3. Materials and Methods

3.1. Materials

We implemented this work using MATLAB version R2020a 64-bit, The MathWorks, Inc., Natick, Massachusetts, United States, 2020. For segmentation, we utilized datasets consisting of 50 Sentinel-2 satellite water bodies and 50 medical images of dermoscopic skin lesions. The Sentinel-2 dataset was obtained from the ESA Sentinel-2 Pre-Operations Hub [5], and it was downloaded from <https://scihub.copernicus.eu> (accessed on 25 July 2022). The dermoscopic skin lesion dataset was sourced from the International Symposium on Biomedical Imaging database (ISBI 2016) [30]. To assess the conceptual validity of our proposed method, we specifically chose sub-datasets characterized by skewed histograms. In these sub-datasets, the Sentinel-2 images exhibited right skewness, while the dermoscopic images displayed left skewness. This selection allowed us to investigate the impact of mean estimation resulting from the Maximum Likelihood Estimation (MLE) of the Gumbel distribution definition.

3.2. Proposed Method

Thresholding-based image segmentation is an important topic in low-level image-processing approaches. It is difficult to analyze the required region in the foreground in the intricate structure of an image. In response to the improvements in the literature, the objective functions of MCET method rely on the estimated means in image regions. With various types of image scenes, images may have different forms of histogram distribution and thus for sub-histogram regions. The classical mean value is an undesirable value for some cases, e.g., an asymmetric distribution of given samples. Therefore, some skewness in a given sample need to be considered for a mean estimation, as shown in Figure 2. In this paper, our samples are values representing the image's histogram such that the definition of the Gumbel distribution is used in terms of using its Maximum Likelihood Estimation. The main aim is to estimate mean values for such skewed histograms. The minimum case of the Gumbel distribution, which is derived from (6), is shown in (7) and (8); this is to estimate the mean values for the object and background samples in a given image.

$$\mu_1 = -\beta_1 \text{Log} \left[\frac{1}{n_1} \sum_{i=1}^t e^{\frac{x_i}{\beta_1}} \right] \quad (7)$$

$$\mu_2 = -\beta_2 \text{Log} \left[\frac{1}{n_2} \sum_{i=t+1}^L e^{\frac{x_i}{\beta_2}} \right] \quad (8)$$

For the maximum case, the above equations become as follows:

$$\mu_1 = \beta_1 \text{Log} \left[\frac{1}{n_1} \sum_{i=1}^t e^{\frac{-x_i}{\beta_1}} \right] \quad (9)$$

$$\mu_2 = \beta_2 \text{Log} \left[\frac{1}{n_2} \sum_{i=t+1}^L e^{\frac{-x_i}{\beta_2}} \right] \quad (10)$$

where μ_1 and μ_2 are the estimated mean values for the first and the second regions, respectively. β_1 and β_2 are the scale values for each region and are estimated from the definition in (5). n_1 and n_2 are the lengths of the first and the second samples, respectively. In our case, they are the corresponding numbers of pixels in image regions.

The proposed approach aims to utilize the estimated mean values derived from the definitions in Equations (7) and (8) when optimizing the objective functions for minimum cross-entropy thresholding. Equation (11) represents the objective function of minimum cross-entropy thresholding (MCET), which enables the examination of both the minimum and maximum scenarios within the context of Gumbel distributions, as illustrated in

Figure 3. This is performed concurrently with the application of other methods using different distributions for the purpose of comparison.

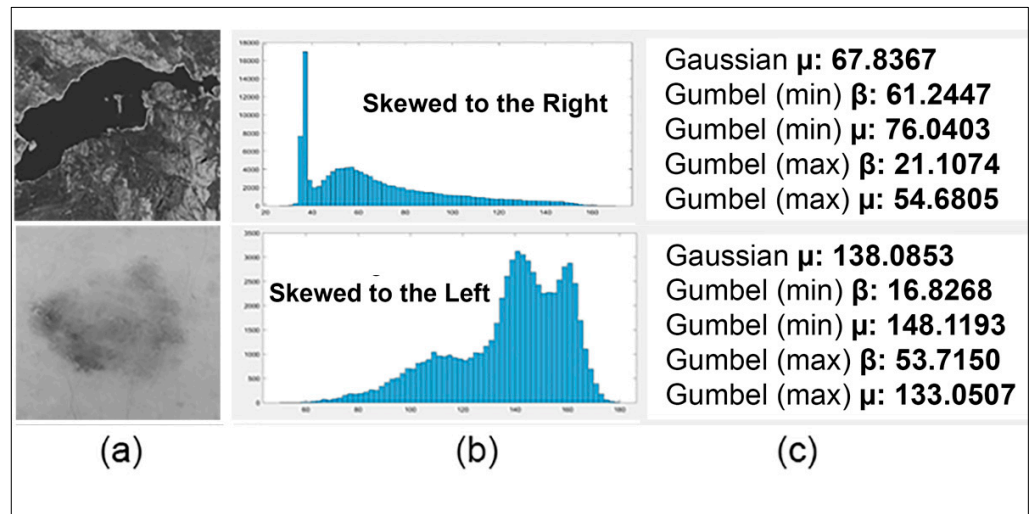


Figure 2. Mean estimation for the selected samples, (a) the Sentinel-2 satellite water body and Dermoscopic ISIC Skin Lesion, respectively. (b) The corresponding histograms and (c) estimated parameters.

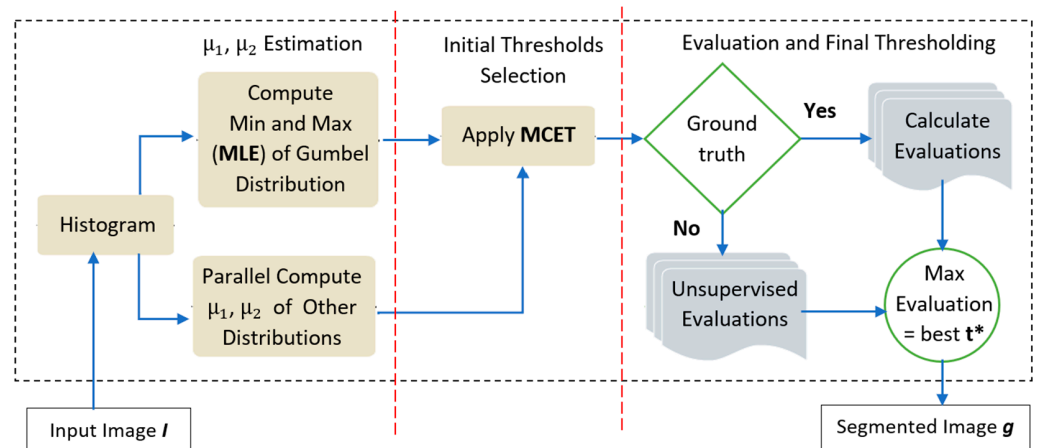


Figure 3. The overall framework of the proposed method.

Other distributions, such as gamma, log-normal, and Gaussian distributions, are employed to represent related works in this context. After the threshold selection process, the evaluation and final thresholding can be achieved using either ground truths present for the segmented images or, if ground truths are missing, unsupervised evaluation, as explained in Section 4.

$$n(t) = -\sum_{i=1}^t ih(i) \log(\mu_1) - \sum_{i=t+1}^L ih(i) \log(\mu_2) \tag{11}$$

where $n(t)$ is the objective function of MCET, $h(i)$ is the histogram of the grey level i in the range $[1, L]$, and μ_1 and μ_2 are the mean values of the first and the second regions of the image, respectively.

3.3. Proposed Algorithm

The computational effort required to determine the value denoted as t^* follows a time complexity of $O(L^2)$ [9]. Nevertheless, when dealing with diverse distributions, the

pursuit of an optimal threshold can prove to be a rather time-consuming endeavor. In the context of an α -thresholding model, the time complexity escalates to $O(L^{\alpha+1})$. To expedite the algorithm's execution, parallel processing emerges as a valuable resource for addressing this challenge. The proposed algorithm was executed using the parallel processing capabilities of Matlab 2019. Consequently, this approach enabled a more efficient execution of the overall computational procedures. The proposed algorithm, as stated in Algorithm 1 and as described in our paper, returns the best threshold values for our proposed method and other relevant methods using parallel processing. The selection of the best threshold value was based on the highest evaluation scores for each method. We calculated these scores by averaging the results of both unsupervised and supervised evaluations for image segmentation, as explained in Section 4.

Algorithm 1 Parallel Processing

1. Input image. I
 2. Compute image histogram $h(i), i = 0, \dots, 255$.
 3. ParFor loop $t = 1:255$ do:
 4. Compute μ_1 and μ_2 and using the definition of Gumbel distribution.
 5. For the minimum case use Equations (7) and (8).
 6. For the maximum case use Equations (9) and (10).
 7. Apply the objective functions of MCET in (11) using the previous μ_1 and μ_2 .
 8. % To compare with other methods:
 9. Apply the objective functions of MCET using Gamma, Gaussian, and Log-normal
 10. Return thresholds t^* for each method. (output segmented images)
 11. End for.
 12. % Evaluation
 13. If ground truths present:
 14. Compute the average sum of unsupervised and supervised evaluations for each output.
 15. Else
 16. Compute the average sum of unsupervised evaluations only for each output.
 17. End if
 18. The best threshold t^* is selected based on the higher evaluation.
 19. Output segmented Image. g resulting from the best t^*
-

4. Performance Evaluation

Checking the optimality of the applied threshold resulting from different techniques provides objective facts for validating the good segmentation result. There are two types of evaluation in this regard: an unsupervised evaluation method that can be used without prior references for the segmented images and the supervised evaluation, which needs references for comparing pixels and matching them with the desired locations in the reference images. A segmentation benchmark for the evaluation ranges between 0 and 1 which reflect poor and precise results, respectively. The best results occur if the evaluation scores are maximized.

4.1. Unsupervised Evaluation

This evaluation depends on the properties of the original image and its associated segmented outcome rather than relying on reference images. This approach is beneficial for segmenting images without established ground truths, e.g., Image Uniformity (IU) and Region Contrast (RC) [25,31,32]. An image uniformity measurement is used to assess the accuracy of the applied threshold, as stated in (12).

$$IU(t) = 1 - \frac{\sigma_1^2(t) + \sigma_2^2(t)}{C} \quad (12)$$

where $\sigma_1^2(t)$ and $\sigma_2^2(t)$ are the variances of the first and the second regions, respectively, and C is computed in (13), and

$$C = \frac{(L_{max} - L_{min})^2}{2} \tag{13}$$

where L_{max} and L_{min} are the maximum and minimum intensity levels.

A region contrast measurement is used to assess the quality of the segmentation by determining whether the segmentation result includes contrast over neighboring, as stated in (14).

$$RC(t) = \frac{|\mu_1(t) - \mu_2(t)|}{\mu_1(t) + \mu_2(t)} \tag{14}$$

where $\mu_1(t)$ and $\mu_2(t)$ are the means of the first and second regions, respectively.

4.2. Supervised Evaluation

This evaluation is dependent on the corresponding references for the segmented images such that it reflects the matching approach between the segmentation result and the required ground truth [33–35]. This evaluation uses specific measurements for pixels classified based on their regions, TN , TP , FP , and FN , as shown in Figure 4.

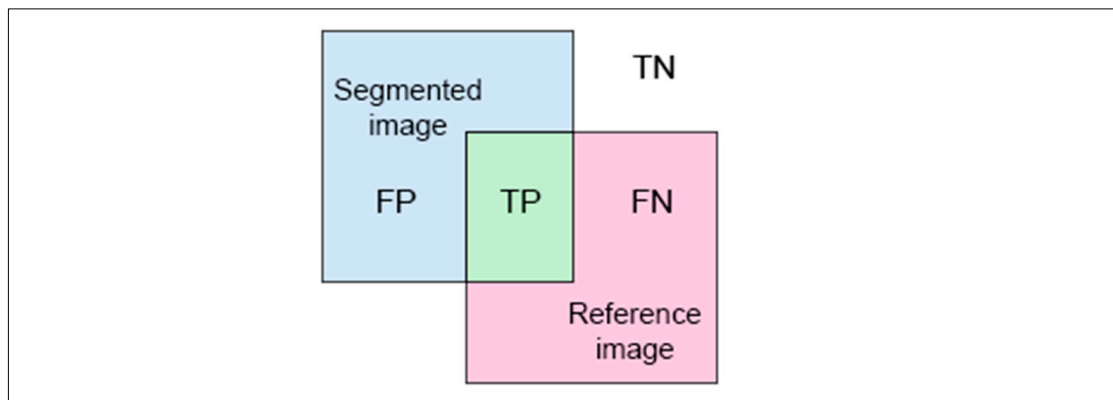


Figure 4. TN are pixels in True Negative or the background and segmented as the background, TP are pixels in True Positive or the object and segmented as belonging to the object, FP are pixels in False Positive or the background and segmented as belonging to the object, and FN are pixels in False Positive or object and segmented as belonging to the background.

A supervised evaluation uses the following metrics.

$$Jaccard_{index} = \frac{TP}{TP + FP + FN} \tag{15}$$

$$F_{Score} = 2 * \frac{Precision * Recall}{Precision + Recall} \tag{16}$$

$$Accuracy = \frac{TP + TN}{FN + FP + TP + TN} \tag{17}$$

$Jaccard_{index}$ is the measurement of the intersection ratio. F_{scores} represents the measurement of the probability of the true positivity such that precision uses the computation of $TP/TP + FP$ and recall uses the computation $TP/TP + FN$. Accuracy is the measurement of the comparison and matching ratio of the pixels from the segmented results and the corresponding references.

5. Results and Discussion

For comparison purposes, we examined the proposed Gumbel-based MCET method and applied the same images as related works that used MCET with different distributions as a distribution-independent thresholding method. The performance measures were calculated by averaging the unsupervised and the supervised evaluations such that the best result among other results depended on the maximum evaluation. The images utilized depicted the necessary skewness for assessing the influence of employing the Maximum Likelihood Estimator (MLE) for the Gumbel distribution in both of its variants. These images were specifically chosen from their datasets as extreme cases, presenting significant difficulties when applying conventional image-segmentation techniques.

As can be noticed in Figure 5, the proposed method has two main objective contributions in segmenting images with skewed histograms compared to related works. Using MCET with the maximum case of the Gumbel MLE showed obvious improvements over related works in segmenting Sentinel-2 Satellite images that demonstrate skewness to the right in their histograms; this applies to the concept of using the maximum Gumbel distribution case with right-skewness samples. Similarly, it is also noticeable that using MCET with the minimum case of the Gumbel MLE showed an improvement in segmenting dermoscopic skin lesion images that demonstrate skewness to the left in their histograms; this applies to the concept of using the minimum case of the Gumbel distribution with the left-skewness samples.

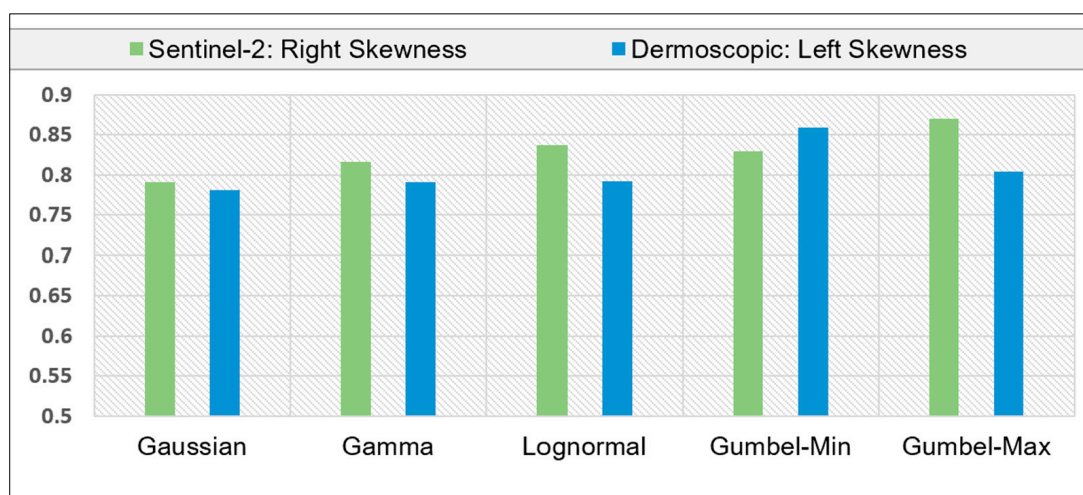


Figure 5. The overall evaluation of the proposed MCET using the Gumbel distribution compared with the related methods' different distributions.

While the Gumbel and log-normal distributions were employed to model the right distribution, the enhancement in segmentation achieved using the Gumbel maximum observed in the proposed method underscores the distinct characteristics of these distributions, which can vary depending on their specific parameters. Using the log-normal distribution in related works has the same concept of the maximum case in handling mean estimation for samples skewed to the right. Although the log-normal method shows an improvement against Gamma, the maximum case of the Gumbel distribution showed an additional improvement in this case; additionally, both cases showed slight improvements in the opposite side of the skewness regardless of their main objective improvement.

As illustrated in Figure 6, the initial pair of images in column (a) depict Sentinel-2 satellite water bodies which exhibit right-skewed histograms. Conversely, the subsequent pair of images portrays dermoscopic skin lesions characterized by left-skewed histograms. As a subjective scene of segmented images, it is noticeable that the similarity of the segmented skin lesions and their reference images was very close when using MCET with the minimum case of Gumbel distribution. It is noticeable that these qualitative results cover

the object of interest in the skin lesions based on objects in the corresponding ground truth. As a quantitative result in Table 1 the corresponding average evaluation scores, 0.85880 and 0.83207, for images (a) 1 and 2, respectively, showed an obvious increase compared to other methods, representing the objective goal in this case and indicating that there is an enhancement in the mean value that positively impacts the objective function of MCET in the left-skewed histogram case.

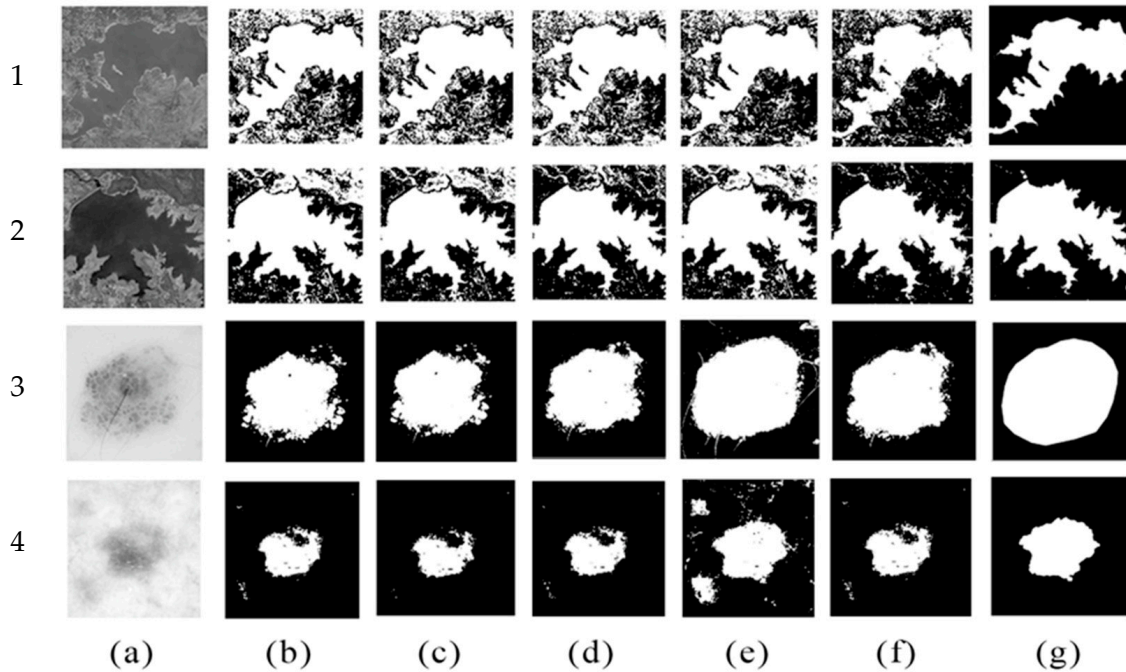


Figure 6. Selected samples: (a) original images, 1 and 2, Sentinel-2 satellite water bodies, and images 3 and 4, dermoscopic skin lesions; (b–f) segmented images using MCET based on the Gaussian [3], Gamma, log-normal [25], Gumbel minimum, and Gumbel maximum, respectively. (g) The corresponding ground truths for the images in column (a).

Table 1. Average evaluation scores of images in Figure 6. (a) Original images’ (b–f) the evaluation of MCET based on the Gaussian [3], Gamma, log-normal [25], Gumbel minimum, and Gumbel maximum, respectively.

	(a)	(b)	(c)	(d)	(e)	(f)
IMG 1		0.79471	0.79471	0.81531	0.80269	0.84069
IMG 2		0.78977	0.81086	0.81966	0.80571	0.85816
IMG 3		0.80253	0.80896	0.80719	0.85880	0.81705
IMG 4		0.75995	0.74663	0.75137	0.83207	0.76492

On the other hand, segmenting the Sentinel-2 images using the maximum case resulted in a similar subjective scene to the corresponding reference images. In Table 1, the evaluation scores, 0.84069 and 0.85816, for images (a) 3 and 4, respectively, reflect an objective improvement in the efficiency of the thresholding objective function based on the new estimated mean in the maximum case.

Table 2 details improvement rates for the proposed method when segmenting right-skewed histograms of the Sentinel satellite water bodies using various distributions. The maximum Gumbel case with MCET stands out with a 10.0% increase over the Gaussian-based MCET and 3.94% over the log-normal method, despite conceptual similarities with the log-normal method. Conversely, for left-skewed histograms, the minimum Gumbel case produced a noticeable improvement rate. It surpasses other distributions with a 9.98%

increase over Gaussian distribution and up to 8.60% over others, as in shown in the rates of Table 3.

Table 2. Improvement rates of the proposed method against different distributions when segmenting images with right-skewed histograms.

Sentinel-2 Waterbodies		
Distributions	Avg. Evaluations	Improvement%
Gaussian	0.79126	--
Gamma	0.81586	+3.10%
Log-normal	0.83740	+5.83%
Gumbel—min	0.82989	+4.88%
Gumbel—max	0.87041	+10.0%

Table 3. Improvement rate of the proposed method against different distributions from segmenting images with left-skewed histograms.

Dermoscopic Skin Lesion		
Distributions	Avg. Evaluations	Improvement%
Gaussian	0.78092	--
Gamma	0.79089	+1.27%
Log-normal	0.79250	+1.48%
Gumbel—min	0.85891	+9.98%
Gumbel—max	0.80419	+2.97%

6. Conclusions and Future Work

In this paper, we introduced a novel approach aimed at improving Minimum Cross-entropy Thresholding (MCET) for image segmentation, particularly when dealing with images exhibiting skewed histogram distributions. Our primary objective is to enhance the estimation of the mean value in such cases. To achieve this, we leveraged the Maximum Likelihood Estimation of Gumbel distributions. We have utilized two variants of the Gumbel distribution, the maximum and minimum cases, and applied them to images with both right and left skewness, respectively. To validate our proposed method's effectiveness, we assessed the quality of the segmented images through both supervised and unsupervised evaluations, depending on the availability of ground truth data for which unsupervised evaluation is particularly valuable when segmenting images lacking corresponding ground truths. As can be seen from the results and their corresponding evaluations, our proposed method outperformed existing techniques that utilize MCET with alternative distribution models, highlighting our approach's efficacy in addressing the challenges of segmenting specific image types.

In future research endeavors, we envision expanding our method's applicability by using heterogeneous skewness in image histograms and integrating it with diverse techniques to construct a versatile segmentation model. This extended model can be employed for various types of images and large datasets for segmentation and object detection purposes.

Author Contributions: This work was based on the efforts of the authors. W.A.H.J. and A.E.-Z.; supervision, A.E.-Z. Conceptualization, W.A.H.J. and A.E.-Z.; methodology, W.A.H.J. and A.E.-Z.; software, W.A.H.J.; formal analysis, W.A.H.J. and A.E.-Z.; investigation W.A.H.J. and A.E.-Z.; resources, W.A.H.J.; writing—original draft preparation and writing—review and editing, W.A.H.J.; visualization, W.A.H.J. and A.E.-Z. All authors have read and agreed to the published version of the manuscript.

Funding: This research received no external funding.

Institutional Review Board Statement: There was no ethical approval for this research since the authors used available datasets from public database, as stated in the manuscript.

Informed Consent Statement: Not applicable.

Data Availability Statement: The data presented in this study are available upon request.

Conflicts of Interest: The authors declare no conflict of interest.

References

- Liang, H.; Jia, H.; Xing, Z.; Ma, J.; Peng, X. Modified grasshopper algorithm-based multilevel thresholding for color image segmentation. *IEEE Access* **2019**, *7*, 11258–11295. [\[CrossRef\]](#)
- Otsu, N. A threshold selection method from gray level histograms. *IEEE Trans. Syst. Man Cybern.* **1979**, *9*, 62–66. [\[CrossRef\]](#)
- Li, C.; Lee, C. Minimum cross entropy thresholding. *Pattern Recognit.* **1993**, *26*, 617–625. [\[CrossRef\]](#)
- Jumiawi, W.A.H.; El-Zaart, A. Otsu Thresholding Model Using Heterogeneous Mean Filters for Precise Images Segmentation. In Proceedings of the 2022 International Conference of Advanced Technology in Electronic and Electrical Engineering (ICATEEE), M'sila, Algeria, 26–27 November 2022; pp. 1–6. [\[CrossRef\]](#)
- Jiang, W.; Ni, Y.; Pang, Z.; Li, X.; Ju, H.; He, G.; Lv, J.; Yang, K.; Fu, J.; Qin, X. An Effective Water Body Extraction Method with New Water Index for Sentinel-2 Imagery. *Water* **2021**, *13*, 1647. [\[CrossRef\]](#)
- Yue, H.; Li, Y.; Qian, J.; Liu, Y. A new accuracy evaluation method for water body extraction. *Int. J. Remote Sens.* **2020**, *41*, 7311–7342. [\[CrossRef\]](#)
- Liu, X.; Hou, S.; Liu, S.; Ding, W.; Zhang, Y. Attention-based multimodal glioma segmentation with multi-attention layers for small-intensity dissimilarity. *J. King Saud. Univ.-Comput. Inf. Sci.* **2023**, *35*, 183–195. [\[CrossRef\]](#)
- Liu, X.; Liu, Y.; Fu, W.; Liu, S. SCTV-UNet: A COVID-19 CT segmentation network based on attention mechanism. *Soft Comput.* **2023**, 1–11. [\[CrossRef\]](#)
- Jumiawi, W.A.H.; El-Zaart, A. A Boosted Minimum Cross Entropy Thresholding for Medical Images Segmentation Based on Heterogeneous Mean Filters Approaches. *J. Imaging* **2022**, *8*, 43. [\[CrossRef\]](#)
- Jumiawi, W.A.H.; El-Zaart, A. Improvement in the Between-Class Variance Based on Lognormal Distribution for Accurate Image Segmentation. *Entropy* **2022**, *24*, 1204. [\[CrossRef\]](#)
- Gumbel, E.J. *Statistics of Extremes*; Columbia University Press: New York, NY, USA, 1958; p. 377.
- Liu, Q.; Huang, X.; Zhou, H. The flexible Gumbel distribution: A new model for inference about the mode. *arXiv* **2022**, arXiv:2212.01832.
- Zhan, Y.; Zhang, G. An Improved OTSU Algorithm Using Histogram Accumulation Moment for Ore Segmentation. *Symmetry* **2019**, *11*, 431. [\[CrossRef\]](#)
- Jumiawi, W.A.H.; El-Zaart, A. Image Spectrum Segmentation for Lowpass and Highpass Filters. In Proceedings of the 2018 4th International Conference on Applied and Theoretical Computing and Communication Technology (iCATccT), Mangalore, India, 6–8 September 2018; IEEE: Piscataway, NJ, USA, 2018; pp. 327–332.
- Kullback, S. *Information Theory and Statistics*; Wiley: New York, NY, USA, 1959.
- Fragoso, R.; Carvalho, M.L.d.S. Estimation of cost allocation coefficients at the farm level using an entropy approach. *J. Appl. Stat.* **2013**, *40*, 1893–1906. [\[CrossRef\]](#)
- Kalyani, R.; Sathya, P.D.; Sakthivel, V.P. Image segmentation with Kapur, Otsu and minimum cross entropy based multilevel thresholding aided with cuckoo search algorithm. *IOP Conf. Ser. Mater. Sci. Eng.* **2021**, *1119*, 012019. [\[CrossRef\]](#)
- Zreika, N.; Zreika, A.; Aref, N.; El Zaart, A.; Al Shakik, A. An improvement of cross entropy thresholding for skin cancer. *BAU J.-Sci. Technol.* **2021**, *2*, 2.
- Xavier, A.; Fragoso, R.; De Belém Costa Freitas, M.; Do Socorro Rosário, M.; Valente, F. A Minimum Cross-Entropy Approach to Disaggregate Agricultural Data at the Field Level. *Land* **2018**, *7*, 62. [\[CrossRef\]](#)
- Babu, A.A.; Rajam, V.M.A. Water-body segmentation from satellite images using Kapur's entropy-based thresholding method. *Comput. Intell.* **2020**, *36*, 1242–1260. [\[CrossRef\]](#)
- Chakraborty, R.; Sushil, R.; Garg, M.L. An Improved PSO-Based Multilevel Image Segmentation Technique Using Minimum Cross-Entropy Thresholding. *Arab. J. Sci. Eng.* **2019**, *44*, 3005–3020. [\[CrossRef\]](#)
- Al-Osaimi, G.; El-Zaart, A. Minimum Cross Entropy Thresholding for SAR Images. In Proceedings of the 3rd International Conference on Information and Communication Technologies: From Theory to Applications, Damascus, Syria, 7–11 April 2008; pp. 1–6.
- Esmaili, L.; Mousavirad, S.J.; Shahidinejad, A. An efficient method to minimize cross-entropy for selecting multi-level threshold values using an improved human mental search algorithm. *Expert Syst. Appl.* **2021**, *182*, 115106. [\[CrossRef\]](#)
- Jumiawi, W.A.H.; El-Zaart, A. Improving Minimum Cross-Entropy Thresholding for Segmentation of Infected Foregrounds in Medical Images Based on Mean Filters Approaches. *Contrast Media Mol. Imaging* **2022**, *2022*, 1–14. [\[CrossRef\]](#)
- Rawas, S.; El-Zaart, A. Precise and parallel segmentation model (PPSM) via MCET using hybrid distributions. *Appl. Comput. Inform.* **2020**. ahead-of-print. [\[CrossRef\]](#)

26. Dawley, S.; Zhang, Y.; Liu, X.; Jiang, P.; Tick, G.R.; Sun, H.; Zheng, C.; Chen, L. Statistical analysis of extreme events in precipitation, stream discharge, and groundwater head fluctuation: Distribution, memory, and correlation. *Water* **2019**, *11*, 707. [[CrossRef](#)]
27. Pratiwi, N.; Iswahyudi, C.; I Safitri, R. Generalized extreme value distribution for value at risk analysis on gold price. *J. Phys. Conf. Ser.* **2019**, *1217*, 012090. [[CrossRef](#)]
28. Kotz, S.; Nadarajah, S. *Extreme Value Distributions: Theory and Applications*; World Scientific: Singapore, 2000. [[CrossRef](#)]
29. El-Shanshoury, G.; Ramadan, A.A. Estimation of Extreme Value Analysis of Wind Speed in the North-Western Coast of Egypt. *Arab. J. Soc. Sci.* **2012**, *45*, 265–274.
30. Gutman, D.; Codella, N.C.; Celebi, E.; Helba, B.; Marchetti, M.; Mishra, N.; Halpern, A. Skin lesion analysis toward melanoma detection: A challenge at the international symposium on biomedical Imaging. *arXiv* **2016**, arXiv:1605.01397.
31. Levine, M.D.; Nazif, A.M. Dynamic measurement of computer generated image segmentations. *IEEE Trans. Pattern Anal. Mach. Intell.* **1985**, *2*, 155–164. [[CrossRef](#)] [[PubMed](#)]
32. Chabrier, S.; Emile, B.; Rosenberger, C.; Laurent, H. Unsupervised Performance Evaluation of Image Segmentation. *EURASIP J. Adv. Signal Process.* **2006**, *2006*, 096306. [[CrossRef](#)]
33. Dice, L.R. Measures of the amount of ecologic association between species. *Ecology* **1945**, *26*, 297–302. [[CrossRef](#)]
34. Alpert, S.; Galun, M.; Brandt, A.; Basri, R. Image segmentation by probabilistic bottom-up aggregation and cue integration. *IEEE Trans. Pattern Anal. Mach. Intell.* **2012**, *34*, 315–327. [[CrossRef](#)]
35. Pont-Tuset, J.; Marques, F. Supervised Evaluation of Image Segmentation and Object Proposal Techniques. *IEEE Trans. Pattern Anal. Mach. Intell.* **2015**, *38*, 1465–1478. [[CrossRef](#)]

Disclaimer/Publisher’s Note: The statements, opinions and data contained in all publications are solely those of the individual author(s) and contributor(s) and not of MDPI and/or the editor(s). MDPI and/or the editor(s) disclaim responsibility for any injury to people or property resulting from any ideas, methods, instructions or products referred to in the content.